ISSN 0389-4010
UDC 621.456.2.022.5
536.246

NAL TR-1126T

TECNICAL REPORT OF NATIONAL AEROSPACE LABORATORY

TR-1126T

Characteristics of Heat Transfer to Nickel Plated Chamber Walls of High Pressure Rocket Combustors

Akinaga KUMAKAWA, Masaki SASAKI,
Kazuo SATO, Fumiei ONO, Hiroshi SAKAMOTO,
and Nobuyuki YATSUYANAGI

October 1991

NATIONAL AEROSPACE LABORATORY

CHOFU, TOKYO, JAPAN

Characteristics of Heat Transfer to Nickel Plated Chamber Walls of High Pressure Rocket Combustors*

Akinaga KUMAKAWA,*1 Masaki SASAKI,*1
Kazuo SATO,*1 Fumiei ONO,*1 Hiroshi SAKAMOTO,*1
and Nobuyuki YATSUYANAGI*1

ABSTRACT

The chamber walls of two water-cooled calorimetric combustors of different chamber lengths were electroplated with nickel of different thickness to investigate decreasing the temperature of the substrate copper wall and prolonging thrust chambers life. Combustion tests were conducted using liquid oxygen (LOX)/gaseous hydrogen, LOX/gaseous methane, and LOX/RJ-1J propellants. The maximum chamber pressure was 12 MPa and the maximum heat flux reached 120 MW/m^2. For both the LOX/hydrogen and LOX/methane propellants, heat flux values measured at the throat section of the nickel plated chambers were 20−30% less than those measured for the bare copper chamber walls. This infers that subcritical microcracks observed within the nickel layer functioned to relax the layer's thermal stress and to cause a higher thermal resistance than expected. On the other hand, the test results of the LOX/RJ1-J propellant showed that the wall material and/or temperature, the presence of hydrogen, and the injection pattern of propellants all affected the characteristics of carbon deposition on the chamber wall. It was also experimentally revealed that at the same mixture ratio the heat flux values in the presence of carbon deposition were lowered by 50% compared to those in the absence of carbon deposition.

Both nickel layers survived approximalely 30 firing tests having a total duration of 600 s. The durability and reliability of the nickel plating were verified, there by showing that a thin layer of nickel plating is useful for decreasing the heat load of high pressure thrust chambers.

Keywords : heat transfer, rocket combustor, nickel plating, thermal resistance, carbon deposition

---

* received 28 June 1991
*1 Kakuda Research Center

概　要

ロケット燃焼器の熱負荷低減及び長寿命化を目的として燃焼器を2台試作し、液酸／ガス水素、液酸／ガスメタンおよび液酸／RJ-1Jを推進剤とする水冷却高圧燃焼試験に供した。試験は最大燃焼圧力12 MPa、最大熱流束120 MW／㎡の範囲で実施した。

液酸／ガス水素、液酸／ガスメタンの燃焼試験において、熱負荷はニッケル層無しに比べて約20～30%低下し、ニッケル層の遮熱性の有効性が示された。このニッケル層の熱抵抗は計算値よりもはるかに大きい値であった。試験後の断面観察からニッケル層の厚さ方向には巨視的な破壊には到らないマイクロクラックが多数生じており、これが熱抵抗増加の主因子と考えられた。ニッケル層の熱抵抗は厚さが異なるにも係わらず、燃焼静圧と良い相関性を示し、燃焼静圧の増加とともに減少したところから、この推定が正しいことを裏付けた。

液酸／RJ-1Jの燃焼試験では、カーボン層の堆積特性に壁材質あるいは壁温の相違、水素添加の有無及び噴射器エレメント形式の相違が大きく影響することがわかった。また、同一燃焼圧力、混合比の条件下では、カーボン層が堆積した場合の熱流束の値は、堆積がない場合の約50%の値まで低下することがわかった。

各ニッケル層は約30回、累積燃焼時間600秒の燃焼試験に供されたが、脱落、剥離等は観察されず、その耐久性及び遮熱性の有効性が示された。

Nomenclature

C*	characteristic velocity
Cg	coefficient of simplified Bartz's equation
F	fuel
hg	hot gas side heat transfer coefficient
k	thermal conductivity
O	oxidizer
O／F	mixture ratio of oxidizer mass flow rate to fuel one
q	heat flux
x	axial distance from throat
Pc	chamber pressure
R	thermal resistance
Tad	adiabatic wall temperature of hot gas
Tsat	saturation temperature of water
ΔTsat	wall superheat
Twg	hot-gas-side wall temperature
t	thickness
ηc^*	characteristic velocity efficiency

Subscript

Cu	copper or copper substrate
cyl.	cylindrical
exp	experimental
f.c.	injector face plate cooling
max.	maximum
Ni	nickel or nickel layer
sat	saturation
th	throat
w	chamber wall
wg	hot-gas-side wall surface

1. Introduction

High pressure liquid rocket engines using liquid oxygen (LOX)/liquid hydrogen and/or LOX/hydrocarbon propellants are being studied for possible use in the next generation of heavy space launch vehicles. Liquid hydrogen, liquid methane, and heavy hydrocarbon of the RP-1 class are the most feasible fuels for these engines. High pressure LOX/hydrocarbon rocket engines with liquid hydrogen as coolant are also feasible to avoid the coking problems of hydrocarbon coolant.

The present authors previously reported the heat transfer characteristics of several propellants, namely, LOX/hydrogen, LOX/methane and LOX/RJ-1J, using water-cooled calorimetric chambers with bare copper chamber walls[1]. They also discussed the thermal resistance of the carbon layer deposited on the copper chamberwalls in the case of LOX/RJ-1J.

Heat fluxes of high pressure chambers are as high as 100 MW/m^2, and with most coolants except liquid hydrogen, it becomes difficult to cool the walls. One way to reduce high heat flux is to use a thermal barrier, such as a ceramic coating, on the hot-gas-side wall. However, the ceramic coating easily causes spalling or flaws under high temperature gradient conditions due to the mismatch of the thermal expansion between the ceramic layer and the metal substrate. Extensive work on ceramic coating systems has been done[2], but these systems are not employed in practical use because of the lack of reliability and durability. Such functionally gradient materials might be promising, but they are still under study[3,4].

Another way to use a thermal barrier is to plate high temperature metal, such as nickel, on the chamber wall. However, thermal conductivity of high temperature metals is higher than that of ceramics. Therefore, a thick coating of the metal is required to obtain high thermal resistance. Such a coating might cause great thermal stress across the coated layer and result in separation of the two metals at their interface. Not much is known about the durability of such plated metals under high heat flux nor about their effective thermal conductivity.

The formation of carbon layer on the thrust chamber wall greatly reduces the heat flux from the combustion gas and thus protects the chamber wall from reaching excessively high temperature. Though the carbon deposition was affected by the combustion gas condition near the wall, it does not affect the combustion phenomena apparently. At this point, it differs from the carbon fouling phenomena in automobile engines and gas turbine engines. The characteristics of carbon deposition are quite complicated and the thermal resistance of the carbon layer deposited on the conventional copper chamber walls was discussed in the previous report[1]. The temperature of a high-temperature-metal coated layer is usually higher than that of the bare copper wall because the coated layer functions as an insulation layer. The characteristics of carbon deposition on the high-temperature surface of the metal plated layer have not been previously examined well.

The effect of hydrogen on carbon formation on nickel and iron surfaces was reported in a laboratory study[5]. However, the carbon deposition characteristics in the presence of hydrogen should be clarified in the case of hydrocarbon-hydrogen dual fuel combustion of hydrogen-

cooled LOX/hydrocarbon rocket engines.

The purpose of this study is, therefore,

(1) to examine the characteristics of heat transfer to nickel plated chamber walls cooled with water by using several propellants, namely, LOX/hydrogen, LOX/methane and LOX/RJ-1J, and

(2) to study the thermal resistance and the durability of the nickel plating using the chamber walls of two water-cooled calorimetric combustors which had different chamber lengths and been electroplated with nickel of different thickness.

2. Experiments

2.1 Injectors

Injectors with 18 coaxial elements were used in LOX/hydrogen and LOX/methane firing tests. Twelve film cooling holes were drilled into the periphery of the regimesh face plate of each injector. The injectors' geometries are shown in Fig. 1 and their operating characteristics are described in Table 1.

Two injectors, 12-elements FOF and OFO impinging types, were employed in LOX/RJ-1J tests. Transpiration cooling with gaseous hydrogen or helium was employed to protect the regimesh face plates of these two injectors. The geometry of the injector with OFO im-

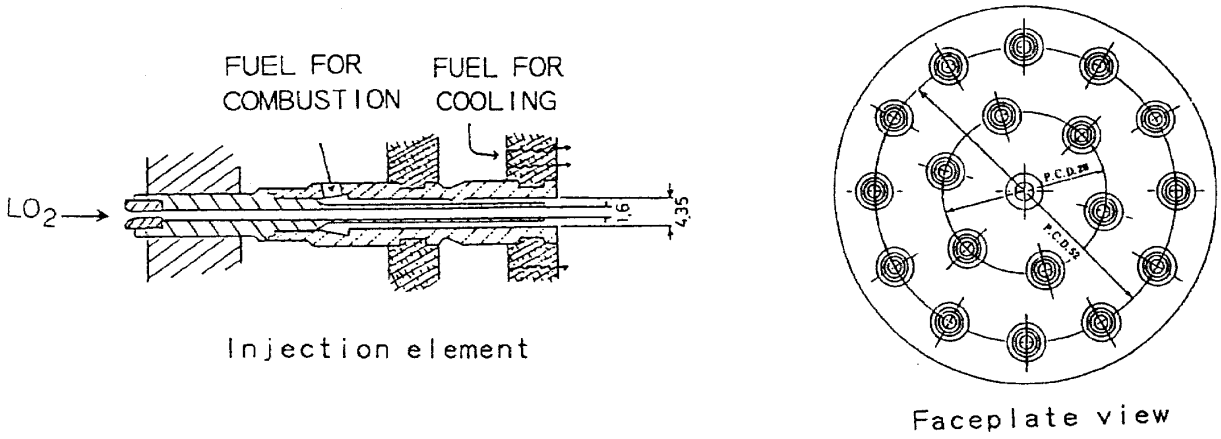

Fig. 1 Injector with coaxial elements

Table 1 Range of Test Conditions

Propellants	Chamber	Injector	Number of Tests	Pc MPa	O/F	ηc^* %
LOX/H^2	23ch.	coaxial	13	2.9 - 9.0	5.8 - 9.9	96 - 99
LOX/CH^4	27ch.	coaxial	8	3.5 - 5.5	2.4 - 4.5	93 - 96
LOX/RJ-1J	23ch.	FOF imp.	14	7.0 - 12.3	2.4 - 3.2	90 - 95
LOX/RJ-1J	23ch.	FOF imp.	3	7.2 - 10.2	2.6 - 2.9	97 - 98
LOX/RJ-1J	27ch.	OFO imp.	19	7.1 - 7.3	2.2 - 3.2	96 - 98

pinging elements is shown in Fig. 2. The pattern and impinging angle of the injector with FOF impinging elements were the same as those of the one with OFO impinging elements. The diameter of fuel holes of FOF elements was 0.9 mm and that of the oxidizer was 1.9 mm.

2.2 Chambers

Two water-cooled calorimetric chambers with nickel plated surface walls were used to measure the axial distribution of heat flux to the chamber wall. They consisted of 23 or 27 circumferential cooling channels, respectively, and had the same inner contours with the exception of the region of the cylindrical section. The length of the 27-channel chamber was 50 mm longer than that of the 23-channel chamber. The geometry of 23-channel calorimetric chamber is shown in Fig. 3.

The fabrication process was as follows:

The cooling channels were machined into an OFHC copper shell and nickel was then plated on the inside wall of the shell. The thickness of the nickel layer shown in Fig. 4 was determined to be between from 0.05 to 0.2 mm in the first trial. The thickness of the nickel layer depended on the plating conditions and it was difficult to get uniform thickness distribution along the axis of the chamber because of the complicated nozzle configuration. The shell was then covered with stainless steel outer rings by means of electron beam welding. The cooling side of the channels had small triangular fins positioned at 30-degree angles in order to enhance heat transfer coefficients on the coolant side.[1]

A water-cooled cavity ring was installed to suppress the combustion instability in cases where LOX/methane and LOX/RJ-1J propellants were used.

Five thermocouples were installed in the chamber wall through the land between the neighboring cooling channels to determine the hot gas side-wall temperature. The two wall thermocouples at the throat section consisted of

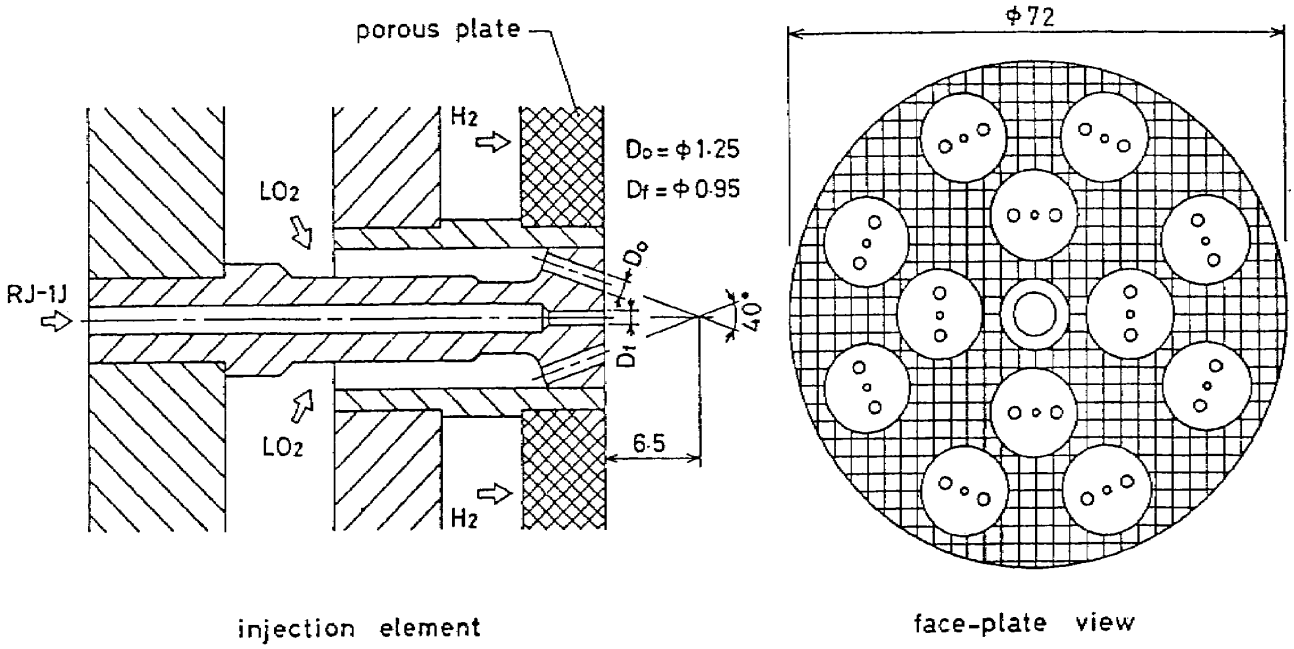

Fig. 2 Injector with OFO impinging elements

a Chromeland Alumel wire 0.045 mm in diameter inside a sheath made of 0.25 mm stainless steel tubing. The other thermocouples consisted of 0.09 mm Chromel/Constantan wire inside a 0.5 mm sheath. Probes were fixed by high thermal conductive epoxy resin at the bottom of drilled holes located 1.0 mm from the hot gas side surface.

The water inlet and outlet temperatures were measured by Chromel/Constantan thermocouples inserted in a inlet manifold and each outlet manifold.

The water flow rate of each channel was measured by a calibrated orifice and the each

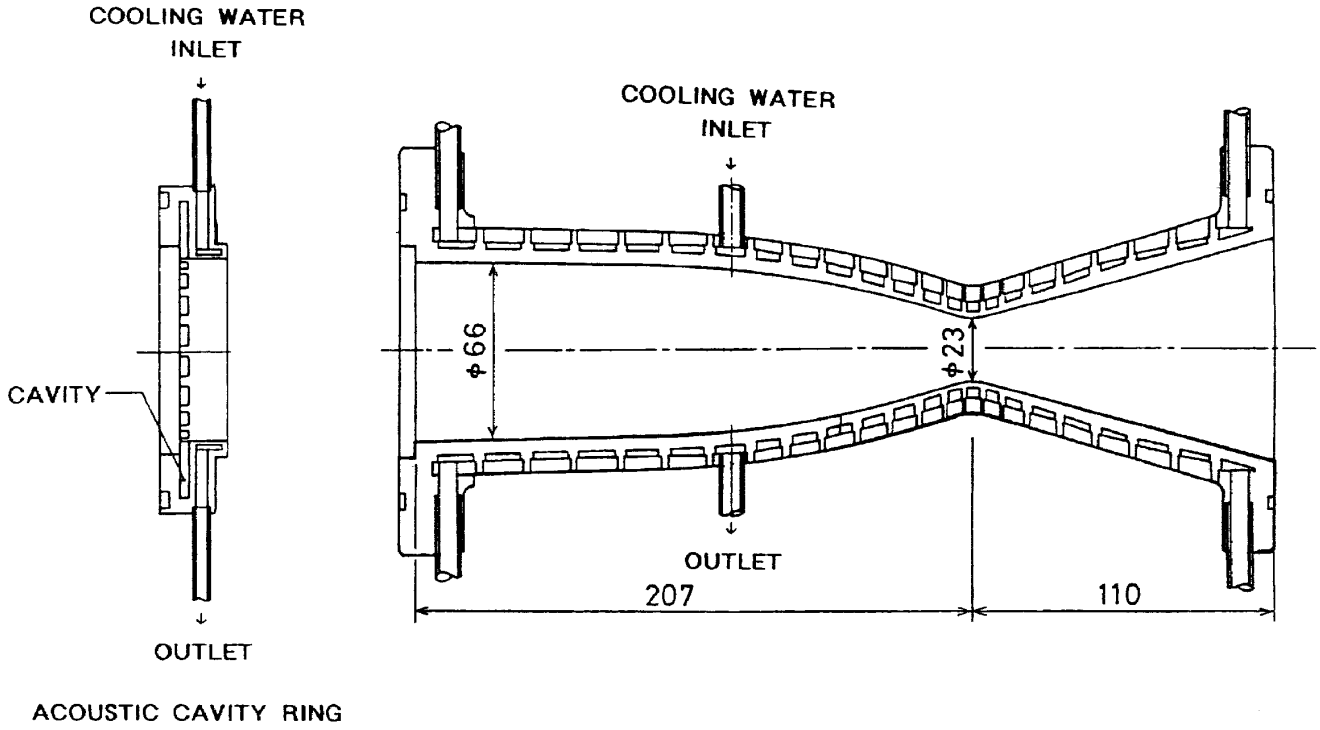

Fig. 3 Water-cooled calorimetric chamber

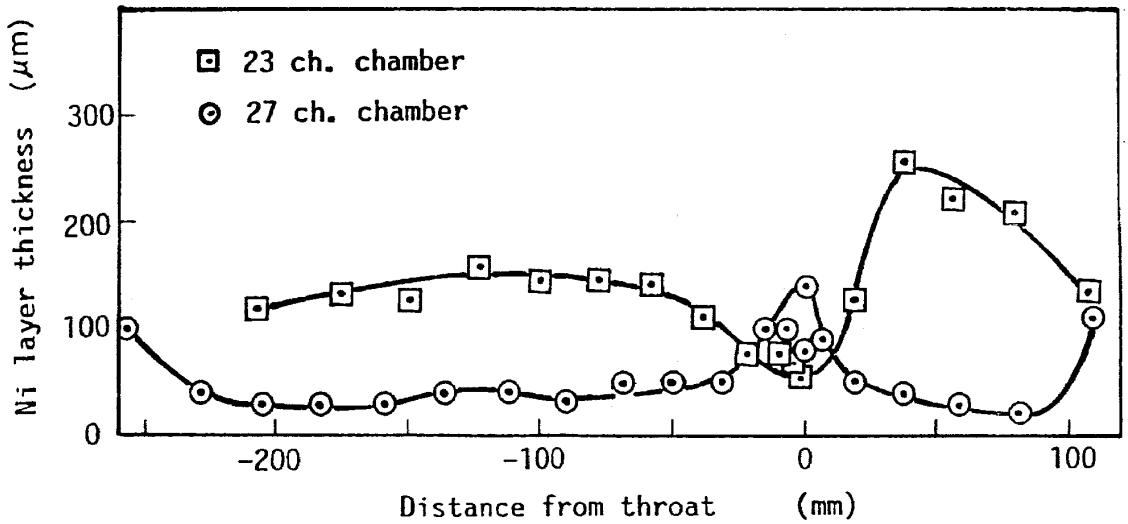

Fig. 4 Axial thickness distribution of nickel plating

propellant flow rate was measured by a turbine flowmeter.

Five pressure transducers were mounted on the cooling channel outer rings to determine the saturation temperature in the cooling channels.

The thrust of the chamber was not measured because of the large quantity of rigid hardware mounted on the test assembly.

2.3 Test Facility

A schematic diagram of the water-cooled combustion test facility is shown in Fig. 5. Details of the test facility are shown in Ref. 1.

3. Test Results

3.1 Test Conditions

Firing tests were carried out, covering a combustion pressure range of 3.5 to 12 MPa and a sea level thrust range of 3 to 7 kN. Test conditions and the achieved C* efficiencies are summarized in Table 1.

At first, the short chamber was used in LOX/room temperature gaseous hydrogen and LOX/RJ-1J combustion tests.

In the LOX/gaseous hydrogen firing tests, the durability of the nickel layer and the thermal resistance of the layer were examined. For exact comparison to study the thermal resistance of the nickel layer as a thermal barrier, combustion tests were carefully conducted under the same conditions as in previous tests[1] in which a 23-channel chamber with a bare copper wall and the same injector was used. Chamber pressures, mixture ratios and

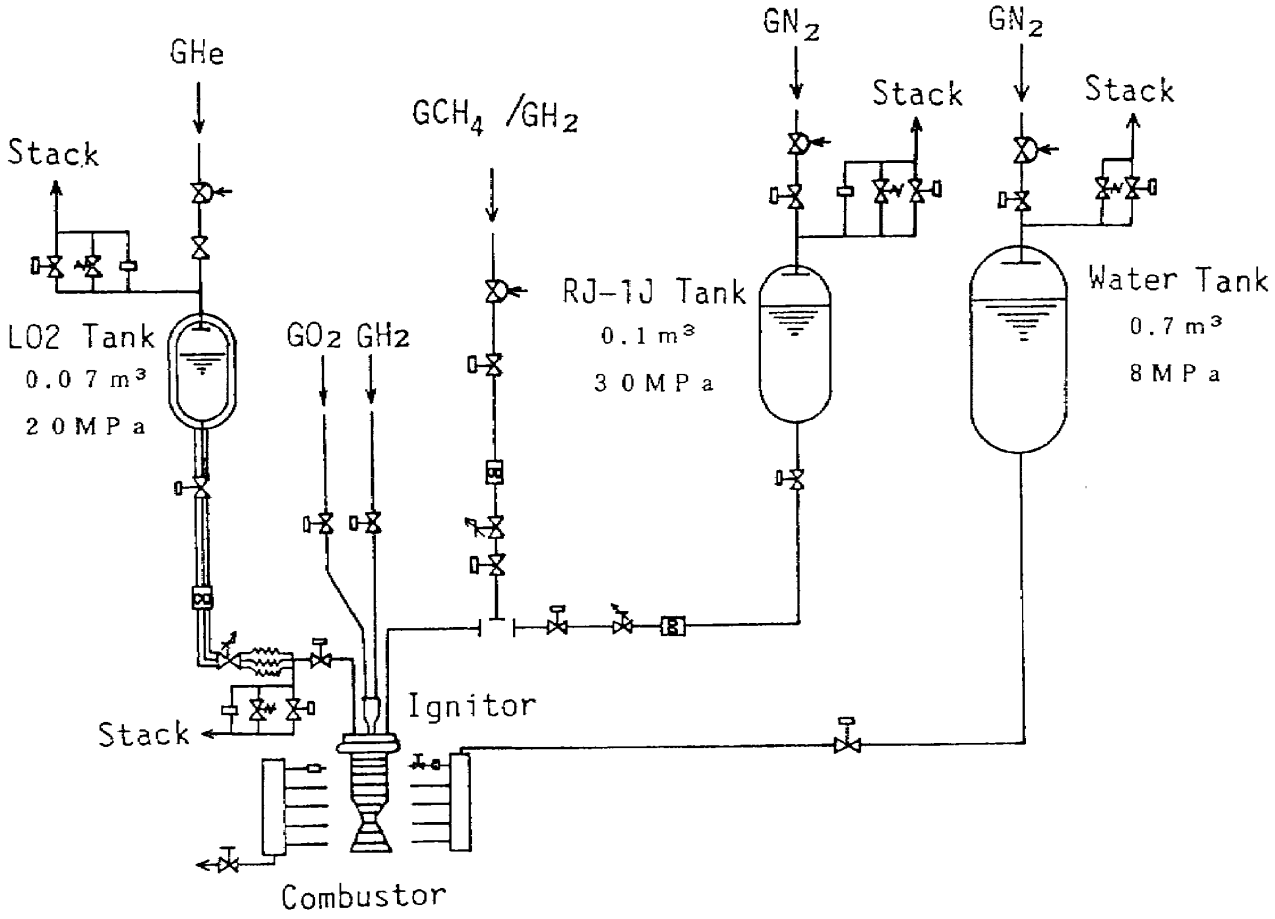

Fig. 5 Schematic diagram of test facility

achieved C* efficiencies of both chambers are shown in Fig. 6; the same combustion and heating conditions were accomplished.

LOX/RJ-1J combustion tests were then conducted. The efficiencies of the two injectors with impinging elements are shown in Fig. 7 individually.

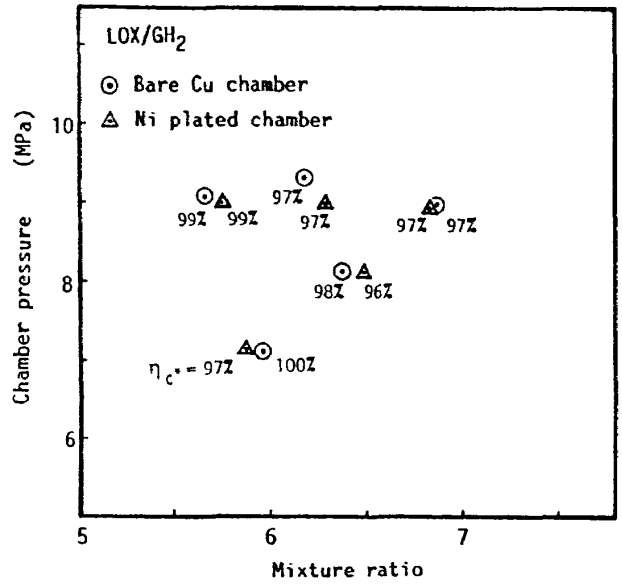

Fig. 6 Experimental region of LOX/GH2 combustion test

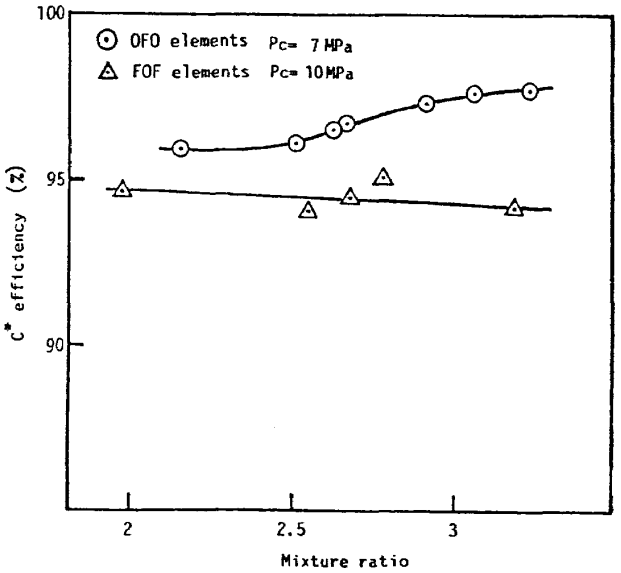

Fig. 7 Measured C* efficiencies of injectors with impinging elements

When the injector with FOF elements was used, the water-cooled cavity ring suffered damage 2 seconds after ignition at a chamber pressure of 12 MPa. The short chamber also suffered melting near the injector end due to high heat flux at a chamber pressure of 10.4 MPa when the OFO impinging injector was used. However, the short chamber plated with nickel survived 30 firing tests with a total duration of 600 seconds.

Combustion tests using the long chamber with 27 cooling passages were then conducted for LOX/RJ-1J and LOX/methane propellants at 3.5 to 7 MPa of chamber pressure. Any carbon deposition was not observed on the nickel plated chamber wall after each combustion test using LOX/methane propellants. Therefore, the heat transfer data of LOX/methane propellants were used to evaluate the thermal resistance of the nickel layers as in the case of LOX/hydrogen in which the wall is apparently clean. The total number of firing tests of the 27-channel chamber was twenty-seven. The long chamber is still in use.

3.2 Post-test Examination of the Nickel Plated Layer

No visible flaws or spalling were observed on the nickel plated surface walls of either cham-

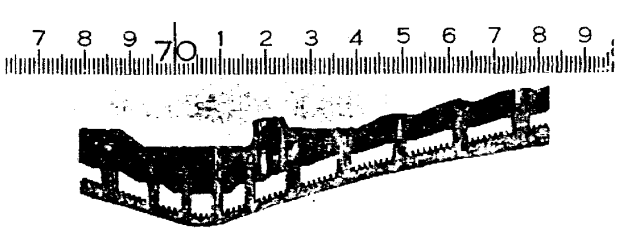

Fig. 8 Cross-section of water-cooled chamber

ber. The 23-channel short chamber was cut in the axial direction to inspect the aspect around the interface between the copper substrate and the nickel layer.

Fig. 8 and Fig. 9 show a cross-section of the cooling channels around the throat section, and Fig. 10 shows a SEM (Scanning Electron Microscope) photograph of this section. Large vertical or inclined cracks were cyclically observed around the throat section as shown in Fig. 9, while there were not any cracks near the injector end and nozzle end. These cracks seem to have been caused by compression stress due to high temperature difference in the axial direction.

Fine cracks were also detected around these macrocracks in the throat section. The interfaces between the copper substrate and the nickel layer were bonded tightly except around the large cracks. It is thought that these subcritical, macro- and micro-cracks were caused by the thermal stress during the start-up of the first combustion test and that they relaxed thermal stress due to the mismatch of thermal expansion of both metals in the following tests and prevented crack propagation. The tightly bonded interfaces except around the large cracks are thought to have prevented spalling of the nickel layer.

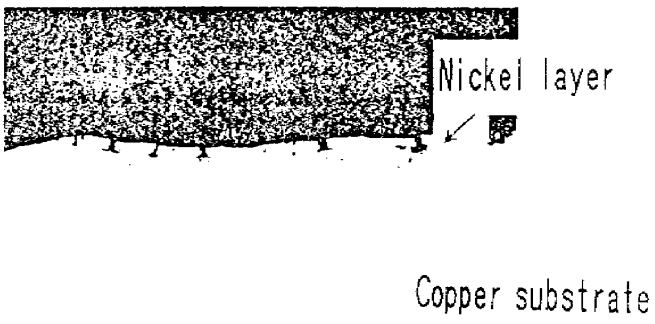

Fig. 9 Cross-section of nickel plated copper wall

3.3 Thermal Resistance of the Nickel Plated Layer

An example of axial heat flux distribution of the 23-channel chamber with a nickel plated layer is compared with that of such a chamber with a bare copper wall in Fig. 11. The measured heat fluxes around the throat section of the nickel plated chamber were about 20% lower than those of the bare copper chamber. However, heat fluxes near the injector and in the nozzle expansion area, where heat fluxes

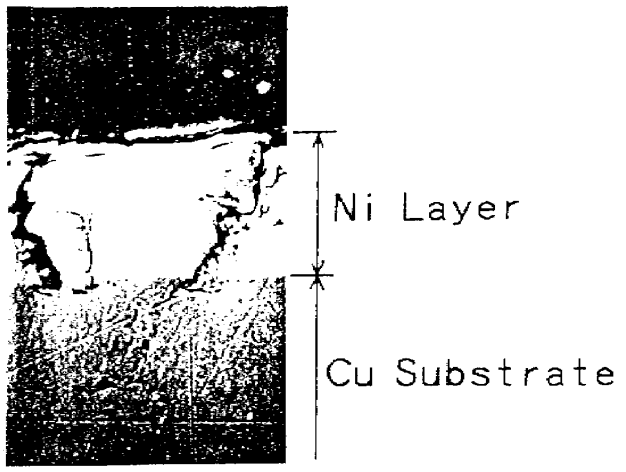

Fig. 10 SEM photograph of cracked nickel plated layer

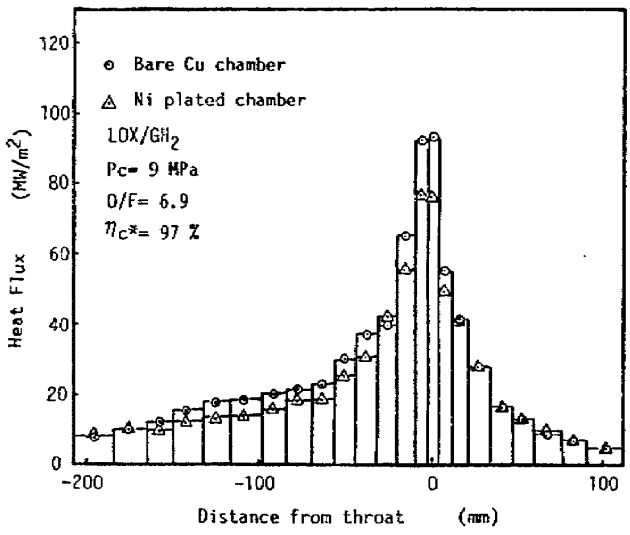

Fig. 11 Heat flux distribution of LOX/GH2 combustion test

are low and no cracks occurred as mentioned above, were almost coincident with each other.

Fig. 12 and 13 are the temperature distributions of both chambers under the conditions shown in Fig. 11. Hot-gas-side copper wall temperatures, Twg_{Cu}, were calculated from measured heat fluxes, q_{exp}, measured water temperatures and pressures, and boiling heat transfer characteristics of 30-degree triangular fins.[1]

$$Twg_{Cu} = T_{sat} + \Delta T_{sat} + q_{exp}\, t_{Cu}/k_{Cu} \qquad (1)$$

The actual hot-gas-side nickel temperature, Twg_{Ni}, was determined by comparison of measured heat fluxes of both chambers considering the effects of variable properties on heat transfer[6].

$$\frac{q_{Ni}}{q_{Cu}} = \frac{hg(Twg_{Ni})(Tad - Twg_{Ni})}{hg(Twg_{Cu})(Tad - Twg_{Cu})} \qquad (2)$$

Hot-gas-side wall temperature of the nickel layer, $T'wg_{Ni}$, was calculated by resolving the one-dimensional, steady-state heat-conduction equation assuming that the nickel layer was in tight contact with the copper substrate.

$$T'wg_{Ni} = Twg_{Cu} + q_{Ni}\, t_{Ni}/k_{Ni} \qquad (3)$$

$T'wg_{Ni}$ and Twg_{Ni} should be essentially coincident with each other if both metals are bonded rigidly and have no defects. However, the

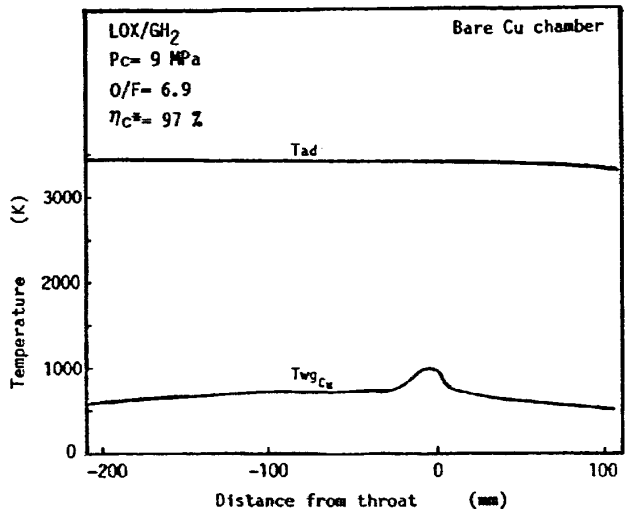

Fig. 12 Wall temperature distribution of LOX/GH2 combustion test with bare copper chamber wall

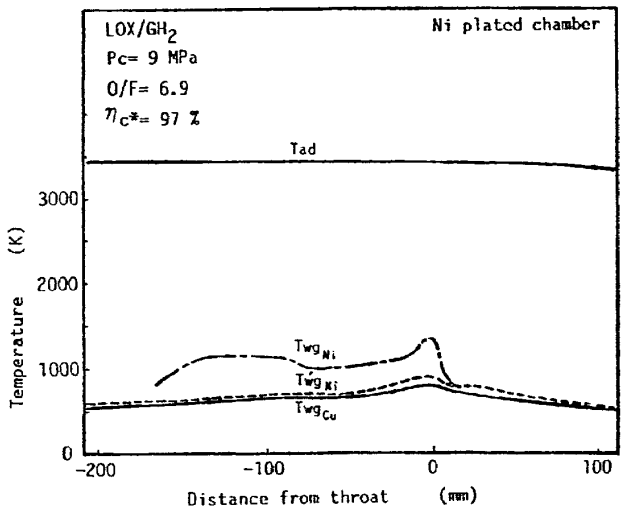

Fig. 13 Wall temperature distribution of LOX/GH2 combustion test with nickel plated chamber wall

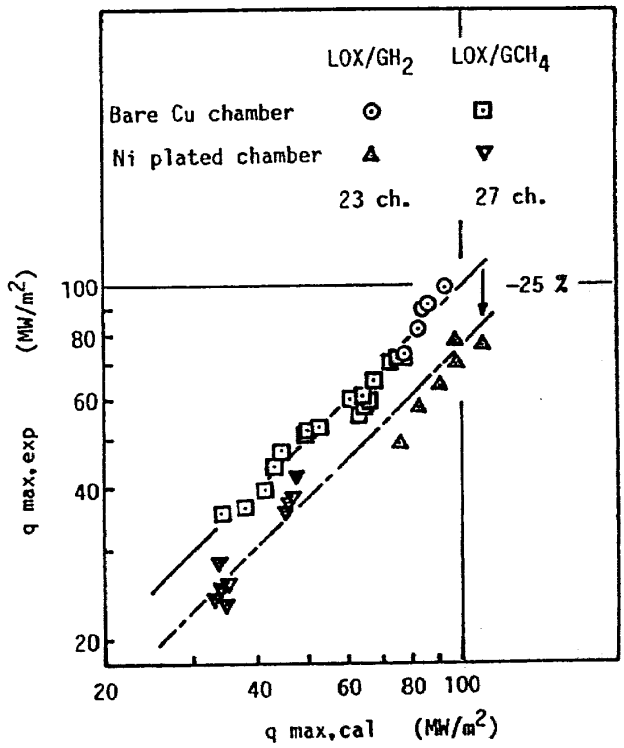

Fig. 14 Comparison of measured and calculated maximum heat fluxes

actual hot-gas-side nickel temperature, Twg_{Ni}, was larger than the assumed hot-gas-side nickel temperature, $T'wg_{Ni}$ around the throat section. This was thought to have been resulted from subcritical cracks around the throat section which acted as thermal resistance.

The heat fluxes measured at the throat section are compared in Fig. 14 with those calculated by the modified Bartz's equation with the coefficient, $Cg=0.023$, which was valid in the cases of LOX/hydrogen and LOX/methane propellants[1]. Measured heat fluxes of the bare copper chamber walls[1] correlated well with values yielded by the modified Bartz's equation as shown in the figure. But the measured values of heat fluxes of the nickel plated chamber walls were 20-30% lower than the calculated values. These differences were thought to be due to the thermal resistance of the nickel layers.

Heat flux ratios, i.e., the ratios of measured heat fluxes and calculated values, were then correlated with static chamber pressures as shown in Fig. 15. The ratios of heat fluxes are almost constant between 0.7 and 0.8 as shown in the figure when the static pressure increased.

Fig. 16 shows the thermal resistance of two nickel plated layers with static pressure at the throat section. The thermal resistance here was defined as follows:

$$\text{Thermal resistance of nickel plated layer} = R_{Ni} = (Twg_{Ni} - Twg_{Cu})/q_{Ni} \quad (4)$$

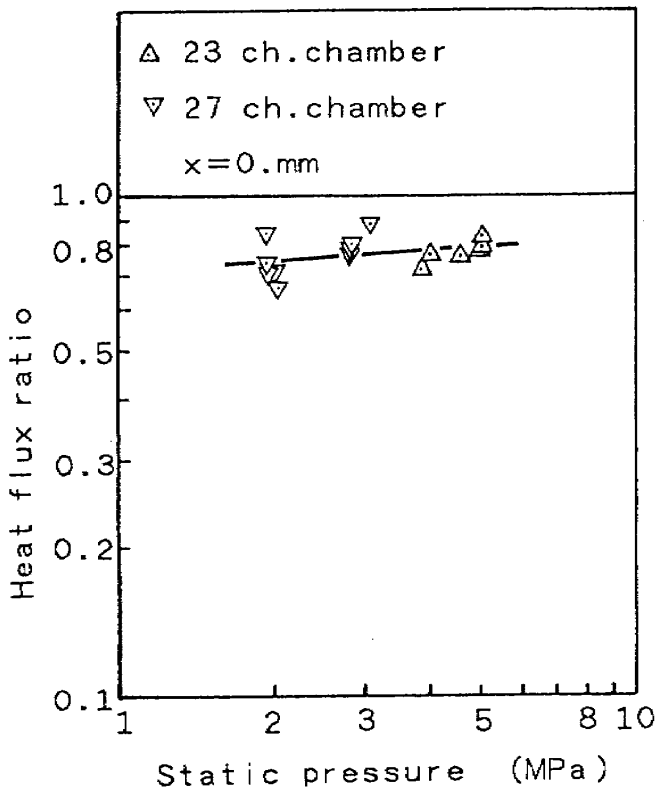

Fig. 15 Heat flux ratios of nickel plated layer correlated with static pressures

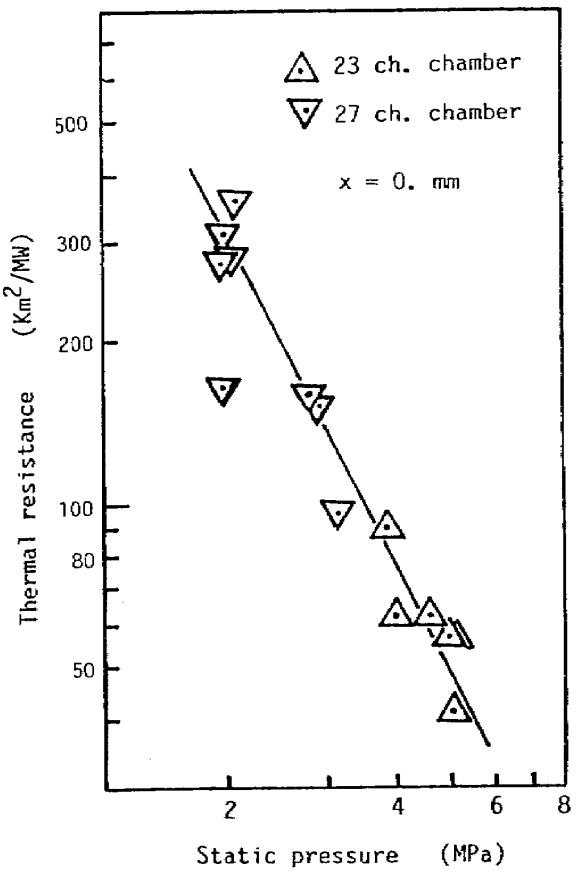

Fig. 16 Thermal resistance of nickel plated layer correlated with static pressures

Though the thicknesses of the two nickel layers are different from each other, good correlation between thermal resistance and static pressure is shown in the figure. As the thermal resistance of solid nickel layers themselves were quite small, i.e., in the range of 1.0 to 1.5 Km^2/MW according to Eq.(4)',

$$\text{Thermal resistance of solid nickel layer} = t_{Ni}/k_{Ni} \qquad (4)'$$

it was inferred that the pores formed by microcracks within nickel layers controlled the thermal resistance between the hot-gas-side wall surface and the nickel-copper interface. Though the ratios of heat fluxes are almost constant between 0.7 and 0.8 as shown in Fig. 15 when the static pressure increased, the thermal resistance of the nickel layer shown in Fig. 16 largely decreased when the static pressure increased. The reason for this phenomenon is considered as follows:

The ratio of heat flux is approximately expressed as,

$$\frac{q_{Ni}}{q_{Cu}} = \frac{hg\,(Twg_{Ni})\,(Tad - Twg_{Ni})}{hg\,(Twg_{Cu})\,(Tad - Twg_{Cu})} \fallingdotseq \frac{1/hg_{Cu}}{(1/hg_{Ni}) + R_{Ni}} \fallingdotseq \frac{1}{1 + hgR_{Ni}} \qquad (5)$$

As R_{Ni} is almost proportional to $Pc^{-2.0}$ shown in Fig. 16 and hg is known to be proportional to $Pc^{0.8}$, hgR_{Ni} in Eq. (5) is proportional to $Pc^{-1.2}$ and the absolute values of hgR_{Ni} are from 0.25 to 0.4 in the experimental range. As a result, the ratios of heat fluxes are almost constant between 0.7 and 0.8 as shown in Fig. 15. It was therefore concluded that the thermal resistance of nickel plated layers decreased when the static pressure increased as the open cracks closed resulting an increase in the contact area.

3.4 Carbon Deposition on the Nickel Plated Layer

Combustion tests of LOX/RJ-1J propellants in the presence of hydrogen were carried out. Two injectors, which had 12 FOF and OFO impinging type elements, were used.

In the case of the FOF impinging type injector, which showed lower C* efficiencies than the OFO type injector, no carbon deposition was observed on the nickel layer in the presence of hydrogen. However, carbon deposition was observed on the wall when gaseous helium rather than hydrogen was supplied. The wall temperatures variations during combustion confirmed these phenomena as shown in Fig. 17 and 18. The wall temperatures variations in Fig. 17 are regarded as being quite small and steady in the presence of hydrogen. However, the fluctuation of the wall temperatures in the presence of helium shown in Fig. 18 is greater than that shown in Fig. 17. This means the carbon layer deposited on the surface wall suffered build-up and spalling during combustion.

Maximum heat fluxes at the throat section with the FOF impinging type injector were almost constant in the presence of hydrogen in the range of tested mixture ratios, while maximum heat fluxes decreased in the presence of helium when the mixture ratio decreased as shown in Fig. 19. These different variations of heat flux were coincident with the observation of the carbon deposition.

However, in the case of the OFO impinging type injector, which showed higher C* ef-

ficiencies than the FOF type injector, carbon deposition was observed on the nickel layer even in the presence of hydrogen. The results are different from those of the FOF impinging type injector as mentioned above. They also differed from those of a previous report[7] in which the injector with OFO impinging elements was used and no carbon deposition was observed in the absence of hydrogen.

Maximum heat fluxes at the throat section with the OFO impinging type injector with 2% hydrogen addition greatly decreased when the mixture ratio decreased as shown in Fig. 19. However, maximum heat fluxes with the FOF impinging type injector with 2% hydrogen addition were almost constant in the experimental range of the mixture ratios though the chamber pressure was 10 MPa, higher than that of the OFO injector, 7 MPa. It was hypothesized that carbon deposition was promoted at lower mixture ratios because fuel rich combustion and larger thermal resistance of the carbon layer at lower mixture ratios resulted in smaller heat fluxes. Based on the experimental data, it was inferred that the heat flux value in the presence of carbon deposition was lowered to 50% of that in the absence of carbon depos-

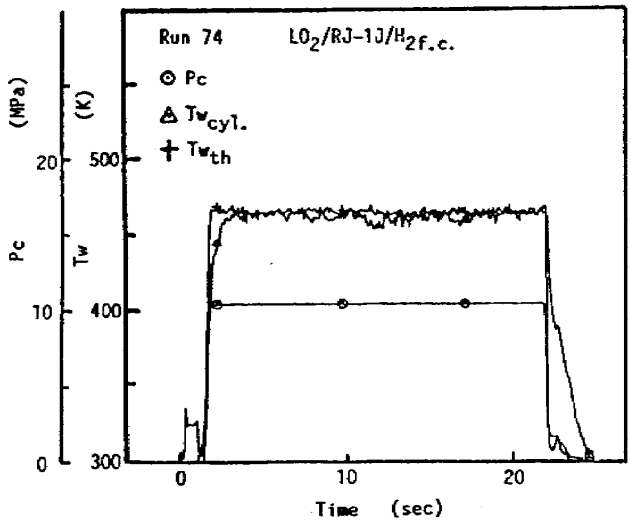

Fig. 17 Wall temperature variation of LOX/RJ-1J combustion test in the presence of hydrogen

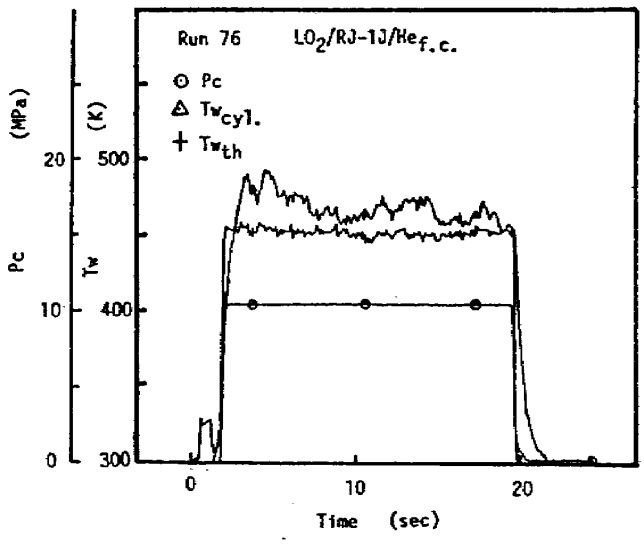

Fig. 18 Wall temperature variation of LOX/RJ-1J combustion test in the presence of helium

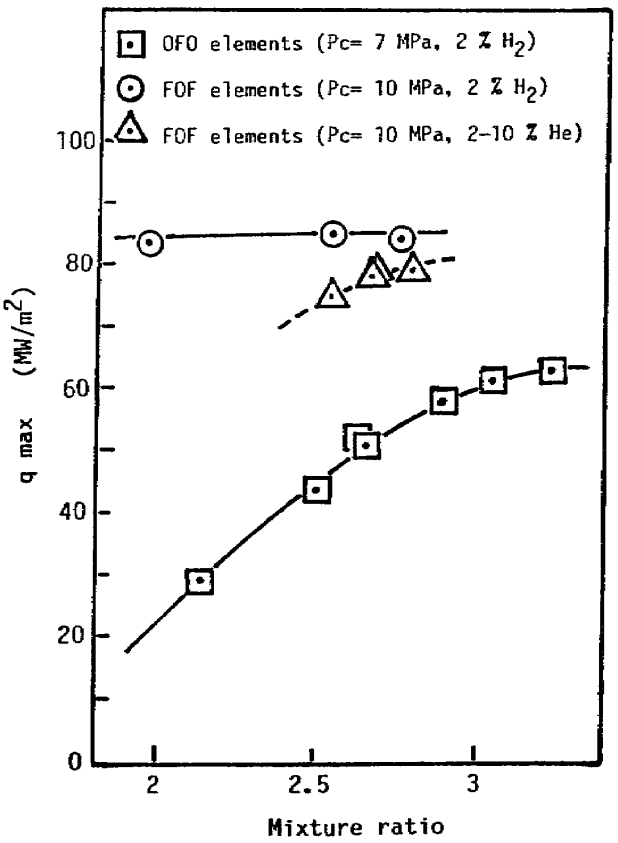

Fig. 19 Measured maximum heat flux of LOX/RJ-1J combustion test as a function of mixture ratios

ition at the same mixture ratio of 2.2 at Pc= 7 MPa.

According to these observations and different variations of heat flux of the two injectors, it is concluded that chemical reaction near the wall surface, the presence of hydrogen, the local mixture ratio, and the resulting wall temperature and/or material compatibility affected the carbon deposition phenomena.

The effects of various factors on carbon deposition are thought to be quite complicated and it is impossible to estimate the thermal resistance of the carbon layer quantitatively at this time. Mass flux of the combustion gas was one such key parameter known as "g model."[1] The effect of the presence of hydrogen, high-wall temperature, material compatibility on carbon deposition and also chemical reaction near the wall surface should be studied in detail in order to understand the carbon deposition phenomena and to "design" optimum thermal resistance of the carbon layer in the future.

4. Conclusion

Combustion tests using LOX/gaseous hydrogen, LOX/gaseous methane and LOX/RJ-1J as propellants were conducted. Two water-cooled calorimetric combustors with nickel plated chamber walls and two types of injectors, a coaxial and an impinging injector, were used. Gaseous hydrogen was added to the hydrocarbon fuel when necessary. The chamber pressure was a maximum of 12 MPa and the heat flux reached a maximum of 120 MW/m^2.

With regard to LOX/hydrogen and LOX/methane propellants, heat flux values measured at the throat section of a nickel plated chamber were 20% to 30% lower than values measured for bare copper chamber walls. It was inferred that microcracks within the nickel layer relaxed thermal stress and prevented crack propagation and that higher thermal resistance of the layer than expected was caused by these microcracks. Tightly bonded interfaces except around the large cracks were thought to have been prevented spalling of the nickel layer.

With regard to LOX/RJ1-J propellants, it was shown that the wall material and/or temperature, the presence of hydrogen and the injection pattern of propellants affected the characteristics of carbon deposition on the chamber wall. It was also experimentally revealed that the heat flux values in the presence of carbon deposition were lowered to 50% of those in the absence of carbon deposition at the same mixture ratios.

The two combustors with nickel plated chamber walls respectively survived about 30 firing tests with a total duration of 600 seconds. The durability and reliability of the nickel plating were verified. It was shown that thin nickel plating is useful to decrease the heat load of high pressure thrust chambers.

References

1. Kumakawa, A., et al., "Hot Gas Side Heat Transfer Characteristics of LOX/H2 and LOX/HC Type Propellants," NAL TR-1062-T, 1990.
2. Quentmeyer, R.J., "Rocket Thrust Chamber Thermal Barrier Coating," NASA CP-2372, 1984.
3. Hirano, T., et al., "An Improvement in Design Accuracy of Functionally Gradient

Material for Space Plane Applications," Proceedings of the 17th International Symposium on Space Technology & Science, Tokyo, 1990.

4. Kumakawa, A., et al., "Experimental Study on Thermomechanical Properties of FGMs at High Heat Fluxes," Proceedings of the 1st International Symposium on Functionally Gradient Materials, Sendai, 1990.
5. Lacava, A.I., "Coke Formation," American Chemical Society, 1982.
6. Bartz, D.R., "A Simple Equation for Rapid Estimation of Rocket Nozzle Convective Heat Transfer Coefficients," Jet Propulsion, 27, (1), 49-51, 1957.
7. Hernandez, R., et al., "Carbon Deposition Model for Oxygen-Hydrocarbon Combustion," NASA CR-179375, 1987.

TECHNICAL REPORT OF NATIONAL
AEROSPACE LABORATORY
TR-1126T

航空宇宙技術研究所報告1126T号(欧文)

平成3年10月発行

発行所 航空宇宙技術研究所
東京都調布市深大寺東町7丁目44番地1
電話三鷹 (0422) 47-5911 (大代表) 〒182
印刷所 株式会社 セイコー社
東京都調布市西つつじヶ丘1丁目5番地15

Published by
NATIONAL AEROSPACE LABORATORY
7-44-1 Jindaijihigashi-Machi Chofu, Tokyo
JAPAN